

Geopolymerisation of low calcium ferronickel slags

K. Komnitsas · D. Zaharaki · V. Perdikatsis

Received: 5 September 2005 / Accepted: 6 June 2006 / Published online: 19 December 2006
© Springer Science+Business Media, LLC 2006

Abstract The present experimental study investigates the feasibility of geopolymer synthesis from low Ca electric arc ferronickel slags. Additives used include kaolinite, sodium silicate, sodium hydroxide and water. The effect of the main factors considered (heating temperature, heating time and aging period) as well as of their interactions on the final compressive strength of the geopolymers produced was studied through a 2^3 factorial design. The experimental results and the variance analysis have shown that only aging period has a statistically very significant and positive effect on the final compressive strength while the effect of the other factors as well as of their interactions were either less significant or negligible. Identification of new phases formed in order to elucidate geopolymerisation mechanisms was carried out by XRD and FTIR. Sodalite, maghemite, thermonatrite, trona and calcite are the major phases identified. The structural integrity of the produced geopolymers was studied by subjecting them to accelerated freeze–thaw cycles. Finally, the durability of the produced geopolymers when immersed in various aquatic and acidic solutions was investigated.

Introduction

Millions of tons of metallurgical slags are produced every year worldwide from several types of furnaces

during nonferrous, ferrous and steel production. Molten slag is usually fast cooled with water forming thus fine grained silicate and glassy phases. Slags were considered in the past as nontoxic and have been used extensively in several applications (harbour-, road construction etc.) Today, the most common use of metallurgical slags is in Portland cement production. The remaining substantial quantities are disposed of in surface disposal sites or under the sea.

Traditional mining and metallurgical waste disposal practices do not often comply with environmental standards for safe disposal and therefore do not guarantee immobilisation of the contained hazardous elements. Solubilisation of these elements under various environmental conditions and subsequent migration through a number of mechanisms endangers the quality of surface- and groundwater causing often severe damages to ecosystems. Therefore, physical and chemical stabilisation of large quantities of mining and metallurgical wastes is necessary. In addition, the implementation of new strict environmental regulations through the adoption of recent EC and other waste management directives [1] requires in most countries the development of an integrated management scheme that prohibits disposal of wastes such as metallurgical slags without a prior detailed environmental characterisation [2]. Since traditional uses of these wastes are expected to be abandoned in the following years the need for the development of new low cost technologies that utilise mining and metallurgical wastes and produce new stabilised products with a potential high added value, such as geopolymers or cements, is expected to increase.

Geopolymers are similar to zeolites in chemical composition but they are characterised by an amorphous

K. Komnitsas (✉) · D. Zaharaki · V. Perdikatsis
Department of Mineral Resources Engineering,
Technical University Crete, Chania 73100, Greece
e-mail: komni@mred.tuc.gr

to semi-crystalline three-dimensional alumino-silicate microstructure [3–5]. Their final structure and physical properties are dependent upon several parameters as water content, particle size, thermal history, alkali metal content and degree of crystallinity or amorphicity [6]. Geopolymers may have permeability similar to Portland cement, close to 10^{-9} cm/s, and may show excellent resistance to acid attack that in some cases surpasses that of cement [7–11]. Compared to concrete, they may also attain higher unconfined compressive strength and shrink less on setting [12, 13]. Other documented properties include good resistance to freeze–thaw cycles [14], as well as immobilisation of most heavy metals contained within the polymeric structure. Some of the possible applications of geopolymers include encapsulation of hazardous wastes and immobilisation of toxic elements such as arsenic, mercury and lead, surface capping of waste dumps, construction of low permeability base liners in landfills, vertical barriers and water control structures, stabilisation of tailing dams, construction of heap leach pads and development of building components that may replace bricks, ceramic tiles and cement [15–17]. In the mining sector geopolymerisation due to fast setting and high early strength acquired may be used during back fill and cut-and-fill operations [18, 19].

The process of geopolymerisation starts with the dissolution of Si and Al in alkaline solutions forming thus a $M_x(\text{AlO}_2)_y(\text{SiO}_2)_z \cdot n\text{MOH} \cdot m\text{H}_2\text{O}$ gel (M: K^+ or Na^+) that after a relatively short setting time hardens [5, 20]. Most proposed mechanisms involve dissolution, transportation or orientation as well as a reprecipitation (polycondensation) step. It should be mentioned though that the exact mechanism of a series of geopolymeric reactions still needs to be elucidated. The synthesis temperature required varies between 20 °C and 80 °C, while the use of pressure is not considered essential [21]. Depending on the synthesis conditions structural integrity and reasonable strength are attained in a very short time, even within 60 min. In most cases, 70% of the final compressive strength is developed within the first 4 h of setting [14].

It is therefore seen that a wide range of natural Al–Si minerals, wastes such as fly ash and various types of slags could serve as potential source materials for the synthesis of geopolymers characterised by high added value, advanced mechanical properties and high acid and fire resistance [22–28]. Reactivity and solubility of the source materials, water content as well as the type of metal silicate used during the synthesis of waste-based geopolymers define to a significant degree the properties of the final products [29]. Previous studies have shown that NaOH dissolves more Al and Si

species from the solid reactants compared to KOH, however, KOH produces geopolymers with a higher compressive strength [19, 30].

Other studies [19, 31, 32] have shown that the calcium content of the raw materials has a significant effect on the final compressive strength. In low alkalinity systems it is possible that both geopolymeric and calcium silicate hydrate (CSH) gels fill the voids and pores of the formed binders [33]. When alkalinity is increased the geopolymeric gel becomes the predominant phase while calcium phases are scattered within the binder. The formation of these gels bridges different hydrated phases and unreacted particles and results in an increase of the mechanical strength of the final product [34].

The use of high calcium slags, such as granulated blast furnace slags, as active filler for the synthesis of fire resistant geopolymers and cements has been extensively studied [14, 34, 35]. In these studies it was shown that setting time correlates well with temperature, potassium hydroxide concentration, metakaolinite and sodium silicate addition. An erosion study of geopolymers containing fly ash and blast furnace slag has shown that their behaviour was similar to that of typical brittle materials. Elastic–plastic indentation events led to the formation of brittle lateral cracks that resulted in loss of material [36].

In the present experimental study the feasibility of geopolymer synthesis from low calcium electric arc ferronickel slags is investigated in order to elucidate the main mechanisms involved. Additives used include kaolinite, sodium silicate, sodium hydroxide and water. The effect of the main factors considered as well as of their interactions on the compressive strength of the geopolymers produced was studied through a 2^3 factorial design [37, 38]. Identification of new phases in order to elucidate geopolymerisation mechanisms was carried out by XRD and FTIR. The structural integrity of the produced geopolymers was studied by subjecting them to accelerated freeze–thaw cycles. Finally, the durability of the produced geopolymers when immersed in various aquatic and acidic solutions was investigated.

Materials and methodology

The waste used in the present study is metallurgical slag derived from an electric arc furnace during ferronickel production at LARCO S.A plant in Greece. The annual slag production is about 1,700,000 t of which approximately 450,000 t is used in the cement industry. Disposal cost of the remaining

quantities reaches 650,000 €/year. The particle size of the as received brittle slag varies between 0.075 mm and 4 mm. Table 1 shows its chemical composition, while the main mineralogical phases as detected by XRD are chromite (FeCr₂O₄), anorthite (CaAl₂Si₂O₈ ~ 20%), magnetite (Fe₃O₄), forsterite (Mg₂SiO₄), fayalite (Fe₂SiO₄ ~ 50%) and christobalite–tridymite (SiO₂).

The slag was crushed using a BICO pulverizer to ~ 0.25 mm. The geopolymers were produced by mixing slag with kaolinite (Fluka), used as inactive filler, sodium silicate solution (Merck, Na₂O:SiO₂ = 3.4, Na₂O = 7.5–8.5%, SiO₂ = 25.5–28.5%) and sodium hydroxide anhydrous pellets (ACS-ISO for analysis). The wt% of the materials used was 69% slag, 9% kaolinite, 4.5% sodium silicate, 4.5% sodium hydroxide (8.3 M) and 13% water. The additives were used to trigger chemical (geopolymeric) reactions between aluminosilicate oxides and alkali metal silicate solutions under highly alkaline conditions that will yield amorphous or semi-crystalline three-dimensional structures consisting of Si–O–Al–O bonds.

First, the solutions were prepared and mixed and then the raw materials were added slowly. After proper mechanical mixing the cement like pulp was cast in cubic moulds (50 mm each side) made of high resistant plastic. Each matrix was vibrated for 5 min so that air trapped within the reactive mass was removed and then placed into a laboratory oven (MMM GmbH) and heated at the required temperature for a specific time. Aging took place under room temperature in order to enhance the development of structural bonds. The compressive strength of the produced geopolymers was measured using a TRI-SCAN 50 load frame.

The main effects and interactions of three main factors, namely heating temperature (factor A), heating time (factor B) and aging period (factor C), on the compressive strength of the final products was studied through a 2³ factorial experiment. The levels of each factor were 60 and 80 °C for factor A, 24 and 48 h for factor B and 7 and 28 d for factor C.

Table 2 shows the experimental factorial design. The signs in each column represent the level of each factor (+ is the high and – the low level) as well as of the interactions AB, AC, BC and ABC (by multiplication of the respective signs). These signs do not have any physical meaning regarding the design and the performance of the experiment. Eight more experi-

Table 2 Design of the 2³ factorial experiment

Treatment combination	A	B	C	AB	AC	BC	ABC
(1)	–	–	–	+	+	+	–
a	+	–	–	–	–	+	+
b	–	+	–	–	+	–	+
ab	+	+	–	+	–	–	–
c	–	–	+	+	–	–	+
ac	+	–	+	–	+	–	–
bc	–	+	+	–	–	+	–
abc	+	+	+	+	+	+	+

ments, under the same conditions seen in Table 2, were carried out in a random order to calculate the experimental error.

Statistical analysis of the experimental data was carried out by the STATGRAPHICS Plus 5 software [39].

XRD analysis of the final products was performed by a Siemens D500 diffractometer using a Cu tube and a scanning range from 3° to 70° 2-theta, with a step 0.03° and 4 s/step measuring time. The qualitative analysis was carried out by the Diffrac^{plus} Software (Bruker AXS) and the PDF data base. FTIR analysis was carried out by the FTIR Spectrometer Model 1000 (Perkin–Elmer) using the KBr pellet technique (0.5 mg powder sample mixed with 250 mg of KBr).

In order to study the durability of the produced geopolymers when exposed to various aquatic and acidic environments specimens produced under the conditions 80 °C, 48 h, 28 d were immersed in solutions containing distilled water, seawater, 1 N HCl and simulated acid rain (H₂SO₄:HNO₃ 60:40 wt%, pH 3) and left for a period of 4 months. Stirring of each solution was done periodically. Fresh solutions were also added periodically to account for evaporation losses. The selection of the solutions was based on common concrete applications. Seawater was used to assess the performance of the produced geopolymers when used in seawater construction works. Acids were used to assess their performance in aggressive industrial environments, including those encountered in the mining and metallurgical sector. Finally, the structural integrity of geopolymers produced under the same conditions was studied by subjecting them to freeze–thaw cycles using –15 and 60 °C as temperature extremes. Compressive strength and change of weight

Table 1 Chemical analysis of ferronickel slag

	FeO	Fe ₂ O ₃	Ni	Co	SiO ₂	CaO	MgO	Al ₂ O ₃	Cr ₂ O ₃	Mn ₃ O ₄	S	C
%	38.8	0.76	0.1	0.02	32.74	3.73	2.76	8.32	3.07	0.44	0.18	0.11

was recorded monthly. In each case control tests were also run. All experiments were performed in duplicate.

Results and discussion

Compressive strength

Statistical analysis of the experimental data was carried out in order to determine the effect of the main factors as well as of their interactions on the compressive strength of the produced geopolymers. The maximum compressive strength measured is 15.78 MPa while the lowest one is 7.53 MPa. The standardised skewness as well as the standardised kurtosis are within the range -2 to $+2$ showing thus that the sample derives from a normal distribution.

A graphical representation of the experimental results is seen in the Box-and-Whisker plot (Fig. 1). The length of the box, which is a measure of variability, represents the interquartile range of the data, which are divided into four areas of equal frequency. The box encloses the middle 50%, where the median is represented as a vertical line inside the box. The mean is plotted as a point. The type of the plot indicates that no outliers are seen. Horizontal lines, called whiskers, extend from each end of the box. The length of the whiskers is also important, so if one whisker is clearly longer than the other, data distribution is probably skewed in the direction of the longer whisker.

Table 3 shows the estimated effects and interactions as well as the standard error using seven degrees of freedom.

The main effects plot, Fig. 2, shows the response variable (compressive strength) as a function of each experimental factor that varies from the lowest to the highest level, while all other factors remain constant at their central values. It can be seen that only the effect of factor C (aging period), with the greatest gradient, is

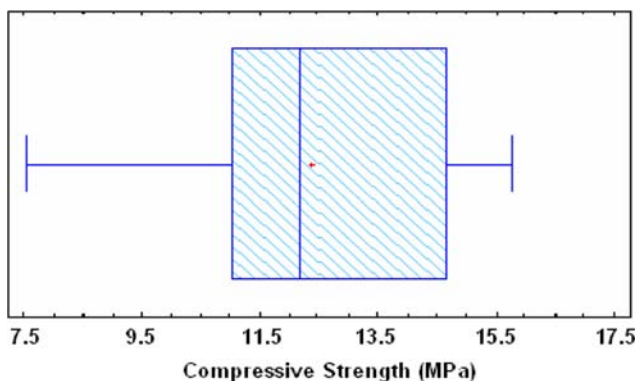


Fig. 1 Box-and-Whisker plot

Table 3 Estimated effects and interactions

Source	Estimated effect	Standard error
Average	12.39	± 0.49
A	0.58	± 0.98
B	1.33	± 0.98
C	3.11	± 0.98
AB	-0.49	± 0.98
AC	0.20	± 0.98
BC	-0.25	± 0.98
ABC	0.16	± 0.98
block	-1.45	± 0.98

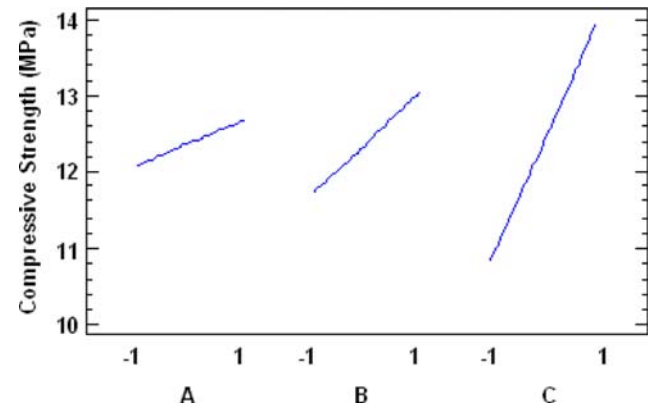


Fig. 2 Main effects plot

considered as statistically very significant and positive. When the aging period increases from 7 d to 28 d the compressive strength increases from 10.8 MPa to 14 MPa, respectively. The effect of factor B—heating time, is positive but less significant, while the effect of factor A—heating temperature is considered as non-significant.

In a similar manner, the interaction plot, Fig. 3, shows the compressive strength as a function of pairs of factors. On one line the second factor is held at its lowest level, while on the other line at its highest level. All other factors, except the two involved in the

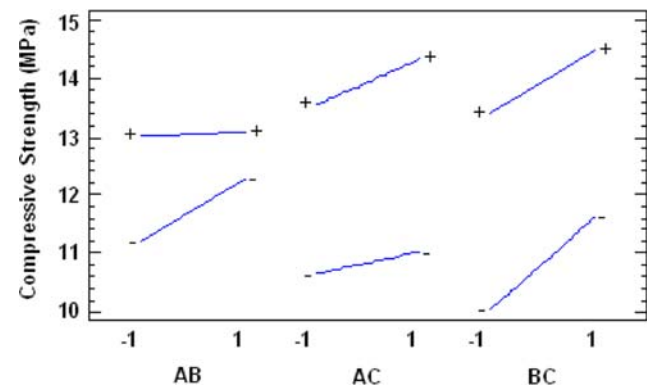


Fig. 3 Interaction plot

interaction under study, are held constant at their central values. It is seen that actually all interactions are considered as less or nonsignificant.

Based on the results of the factorial experiment and the determination of main effects and interactions, the compressive strength of the produced geopolymers can be precisely predicted by the following simple regression equation including only significant effects, namely factors C (aging period) and B (heating time).

$$Y : 12.39 + (1.33/2) * X_2 + (3.11/2) * X_3$$

where Y , compressive strength (true response); 12.39, mean value of compressive strength; 1.33, main effect of factor B; 3.11, main effect of factor C.

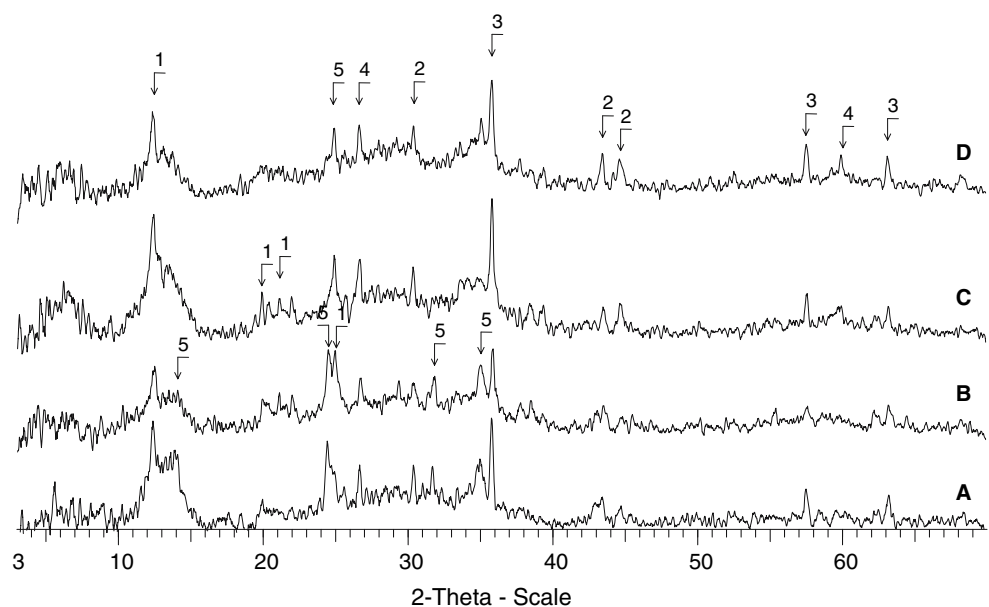
X_2, X_3 : -1 or +1, level of each factor B and C. Other effects and interactions are considered negligible and therefore are not taken into account.

Based on the results of the factorial experiment it is seen that the optimum experimental conditions, in terms of the attained compressive strength, for the synthesis of ferronickel slag based geopolymers are: heating temperature 80°C, heating time 48 h and aging period 28 d. Previous studies show that if the heating temperature is decreased (40°C), the compressive strength decreases as well [40].

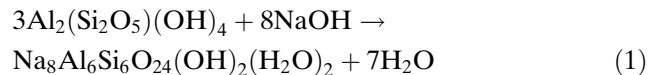
Mineralogy

XRD analysis of the produced geopolymers (Fig. 4) reveals the presence of quartz, kaolinite, magnetite and the formation of synthetic sodalite and maghemite.

Fig. 4 X-ray diffractograms of geopolymers produced under various conditions (A: 60 °C–24 h–7 d, B: 60 °C–24 h–28 d, C: 60 °C–48 h–28 d, D: 80 °C–48 h–28 d, 1: Kaolinite, 2: Maghemite, 3: Magnetite, 4: Quartz, 5: Sodalite)



Sodalite, $\text{Na}_4\text{Al}_3(\text{SiO}_4)_3\text{Cl}$, is a member of the feldspathoid group and belongs to rock forming minerals. Its Mohs hardness varies between 5.5 and 6. It is believed that sodalite contributes to the increase of the compressive strength of the final products. Synthetic sodalite, $\text{Na}_8\text{Al}_6\text{Si}_6\text{O}_{24}(\text{OH})_2(\text{H}_2\text{O})_2$, is produced by replacing Cl^- with OH^- when NaOH reacts with kaolinite according to reaction (1)



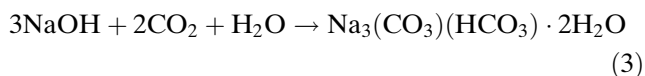
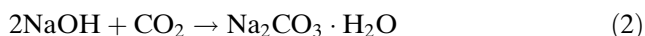
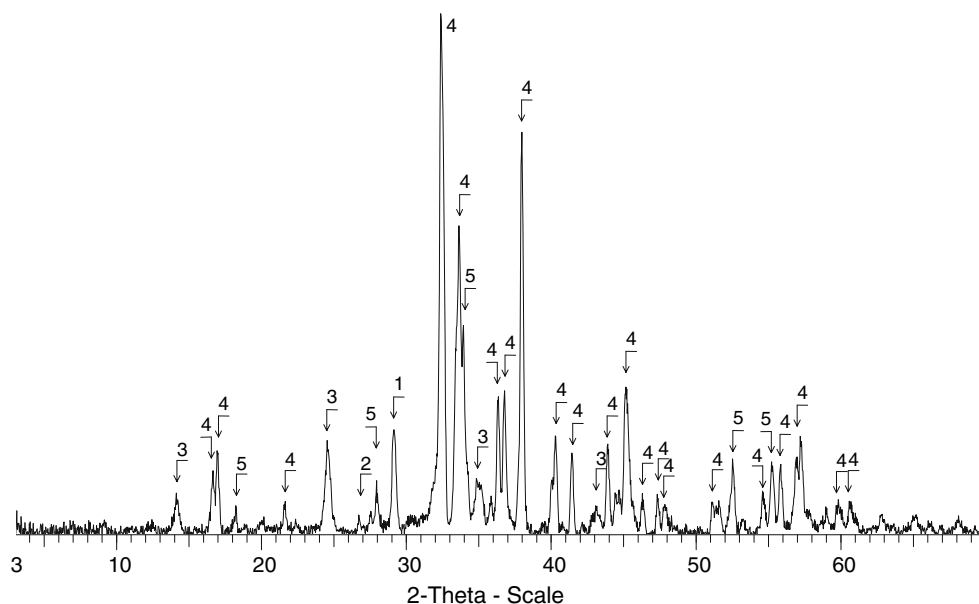
The presence of kaolinite in the produced geopolymers suggests that the initially used quantity has not fully reacted during geopolymerisation.

Maghemite, $\gamma\text{-Fe}_2\text{O}_3$, is formed by weathering or low-temperature oxidation of spinels containing ferrous iron. Maghemite may be also formed relatively easy from goethite on acid sulphate soils [41].

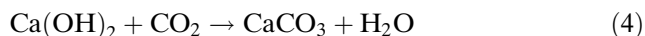
It has to be mentioned that traces of a salt like phase were seen on the surface of geopolymers produced under the conditions 80 °C, 48 h, 28 d. Analysis of this phase revealed the presence of thermonatrite, trona, calcite, sodalite and quartz (Fig. 5).

Thermonatrite, $\text{Na}_2\text{CO}_3 \cdot \text{H}_2\text{O}$, a member of the “soda minerals” group, is formed by atmospheric carbonation of the excess sodium hydroxide, according to reaction (2). The other five minerals of the group are trona $\text{Na}_3(\text{CO}_3)(\text{HCO}_3) \cdot 2\text{H}_2\text{O}$, natrite $\text{g-Na}_2\text{CO}_3$, nahcolite NaHCO_3 , natron $\text{Na}_2\text{CO}_3 \cdot 10\text{H}_2\text{O}$ and wegscheiderite $\text{Na}_2\text{CO}_3 \cdot 3\text{NaHCO}_3$. Trona is produced according to reaction (3)

Fig. 5 X-ray diffractogram of salt like phases formed on the outer surface of the geopolymers produced under conditions 80 °C–48 h–28 d (1: Mangano-calcite, 2: Quartz, 3: Sodalite, 4: Thermonatrite, 5: Trona)



Calcite, CaCO_3 , is formed when calcium hydroxide reacts with atmospheric carbon dioxide according to simple reaction (4).



It is well known that the solubility of calcium decreases at elevated pHs due to the formation of unstable calcium hydroxide. Excess of calcium hydroxide in the geopolymer mixture induces the process of carbonation deteriorating thus the strength of the final product.

It should be underlined that the initial volume of the water used as well as the amount of hydrated phases formed affects the final strength of the geopolymers. If excess water is used or water is not consumed during hydration, free water will diffuse or evaporate if heating temperature is high and therefore pores and cracks will develop and salt like phases will be formed on the surface of the products.

The FTIR Spectra of four geopolymers as well as of the initial slag are seen in Fig. 6. The difference in absorption frequencies for the slag and the final products indicates the transformations that take place during geopolymerisation. The bands at $\sim 530 \text{ cm}^{-1}$ are due to out of plane Si–O bending, while the bands at

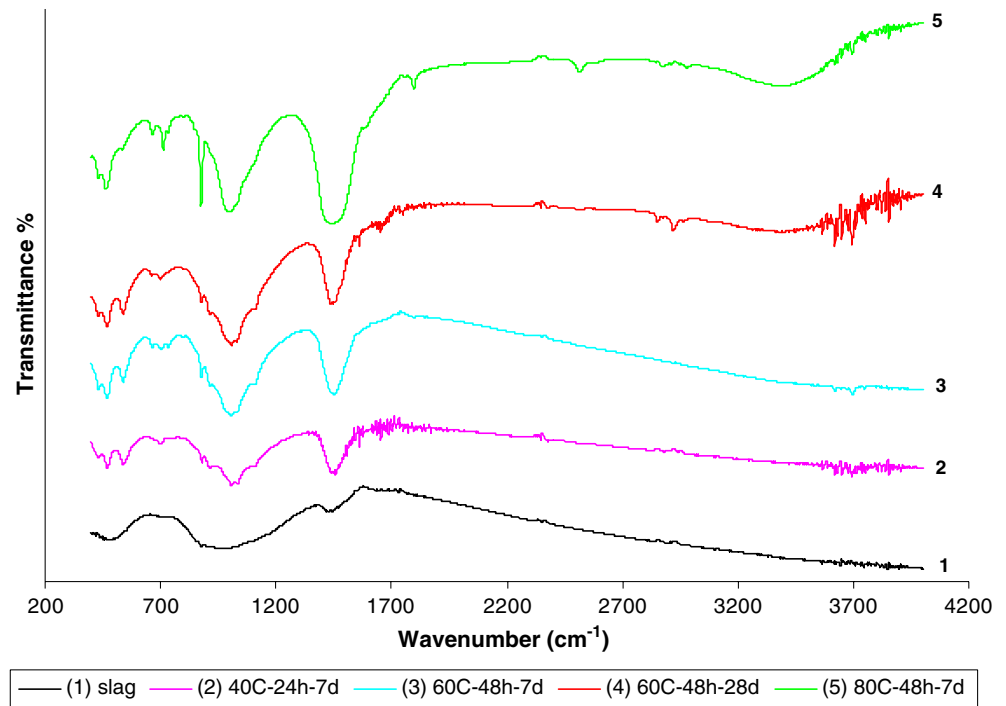
$450\text{--}465 \text{ cm}^{-1}$ are due to in plane Si–O bending and Al–O linkages originating from within individual tetrahedra [29]. Bands at approximately 680 cm^{-1} represent the functional group of AlO_2 . Tetrahedral aluminium can be also detected by the presence of small bands at $\sim 800 \text{ cm}^{-1}$ which are due to symmetric Al–O stretching [26]. The change in the co-ordination number of Al from 6 to 4 generates peaks at 850 cm^{-1} [29].

The broad band of slag at around 942 cm^{-1} has been shifted in geopolymers to around 990 cm^{-1} due to the T–O–Si (T: Si or Al) stretching vibration ($950\text{--}1,200 \text{ cm}^{-1}$). This is probably due to TO_4 reorganisation that takes place when geopolymers are constructed from slag. The bands at $1,088$ and $1,094 \text{ cm}^{-1}$ that are a major fingerprint for the geopolymer matrix and define the extent of polysialation or aluminium incorporation while lowering the energy of the band, are either assigned to asymmetric stretching of Al–O and Si–O bonds originating from within individual tetrahedra [42] or to quartz present in the pastes [43]. The large bands at around $1,450 \text{ cm}^{-1}$ are due to carbonation [44] or due to the presence of Na_2CO_3 . If excess concentration of Na is used part of it is carried to the surface where it then carbonates [45]. The small band seen at $2,504 \text{ cm}^{-1}$ after heating in $80 \text{ }^\circ\text{C}$ is probably due to the infrared band position of HCO_3^- ion [46].

Durability studies

The durability of the geopolymers produced under the conditions $80 \text{ }^\circ\text{C}$, 48 h, 28 d and exposed to various aquatic and acidic environments as well as when

Fig. 6 FTIR spectra of raw slag and geopolymers produced under various conditions



subjected to weekly freeze–thaw cycles over a period of 4 months, in terms of compressive strength and weight change, is seen in Figs. 7 and 8. The final weight was recorded after removing the specimen from solution and drying it for 30 min in room temperature.

From Figs. 7 and 8 it is seen that:

- The compressive strength for the control specimen increases slightly with time and reaches after 4 months 17 MPa. Slight decrease of the compressive strength is seen for the specimens subjected to freeze–thaw cycles or immersed in distilled or seawater. The respective values after 4 months are

14.12, 13.35 and 13.39 MPa. A more remarkable decrease of the compressive strength is seen for the specimens immersed in 1 N HCl and simulated acid rain. In both cases geopolymers lose almost 20% of their compressive strength (11.59 and 11.89 Mpa, respectively).

- Geopolymers immersed in HCl solution, had a clear change in appearance while softening of the outer surface was seen due to the formation of a gel like phase (probably amorphous silica). No change in appearance was seen for the other specimens. The loss of strength is due to depolymerisation of the aluminosilicate matrix in acidic media and the

Fig. 7 Change in compressive strength of geopolymers produced under the conditions 80 °C, 48 h, 28 d, exposed to various aquatic and acidic solutions and subjected to weekly freeze–thaw cycles over a period of 4 months

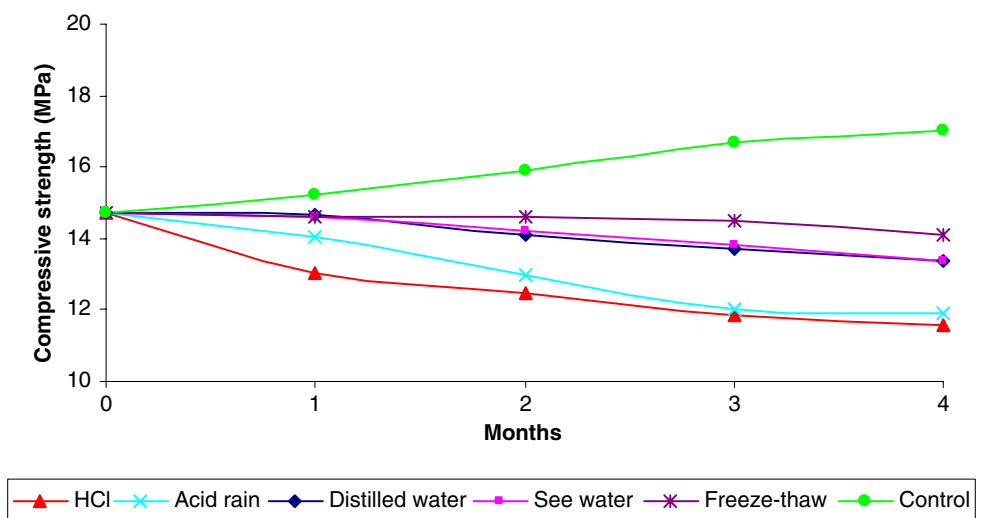
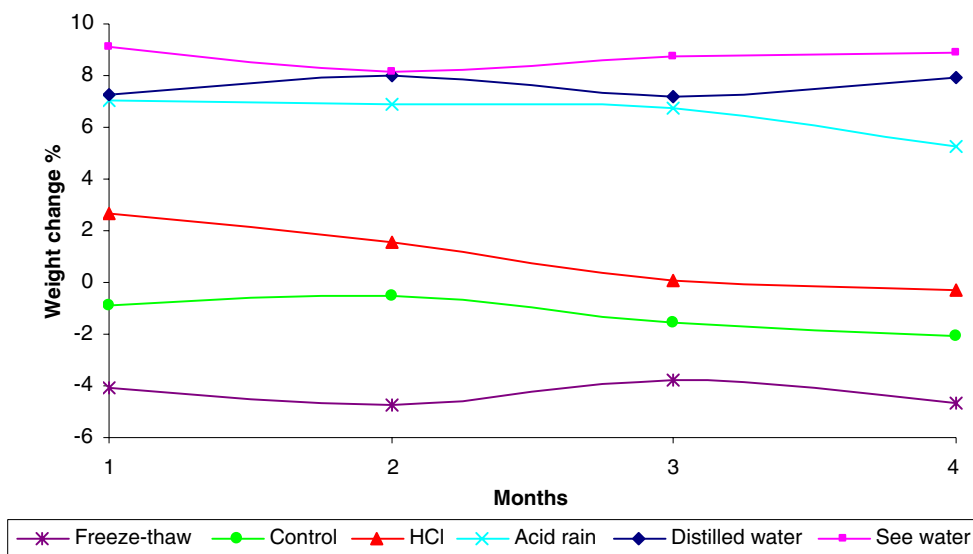


Fig. 8 Change in weight of geopolymers produced under the conditions 80 °C, 48 h, 28 d, exposed to various aquatic and acidic solutions and subjected to weekly freeze–thaw cycles over a period of 4 months



formation of zeolites that also results in loss of weight. Acids cause breakage of the Si–O–Al bonds, dealumination, liberation of silicic acid and partial decomposition of the geopolymer. Depolymerisation is induced by neutralisation of the NaOH with the acid present that results in drop of pH. In addition, H⁺ or H₃O⁺ ions may replace Na⁺ altering thus the condensation process.

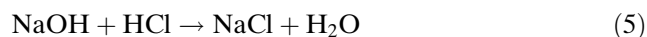
- The solution attack, except for HCl, is mainly restricted on the surface of the specimens. This may indicate passivation of the outer surface due to the formation of reaction products, so that diffusion becomes the rate-limiting step. A similar conclusion was drawn when the solubility of lead slag particles was studied in seawater [2].
- The above conclusions are justified by the minor weight loss for the control as well as for the specimens subjected to freeze–thaw cycles over a period of 4 months (5.7% and 4.6%, respectively). Specimens immersed in distilled or seawater showed a weight increase ranging between 8% and 9%. Specimens immersed in simulated acid rain showed after an initial increase a noticeable loss of weight the fourth month. Finally, specimens immersed in 1 N HCl, showed after a slight initial increase a continuous weight loss (Fig. 8).

Similar results were derived from another study that examined the performance of metakaolin based cementitious materials immersed in 0.001 M sulfuric acid, deionised water, sodium sulfate solution and seawater [47].

XRD analysis of the surface of the specimens tested for durability and integrity reveals the presence of quartz, kaolinite, fayalite, maghemite, sodalite and the

formation of halite, magnesium calcite, calcite, aragonite and akermanite (Fig. 9).

Halite, NaCl, was mainly detected in the outer surface of the specimens immersed in 1 N HCl solution and secondary in seawater. Halite is usually found in evaporative deposits, where it crystallises out of evaporating brine lakes or in ancient bedrock where large extinct salt lakes and seas have evaporated millions of years ago, leaving thick deposits of salt behind. Its formation is attributed to reaction (5).



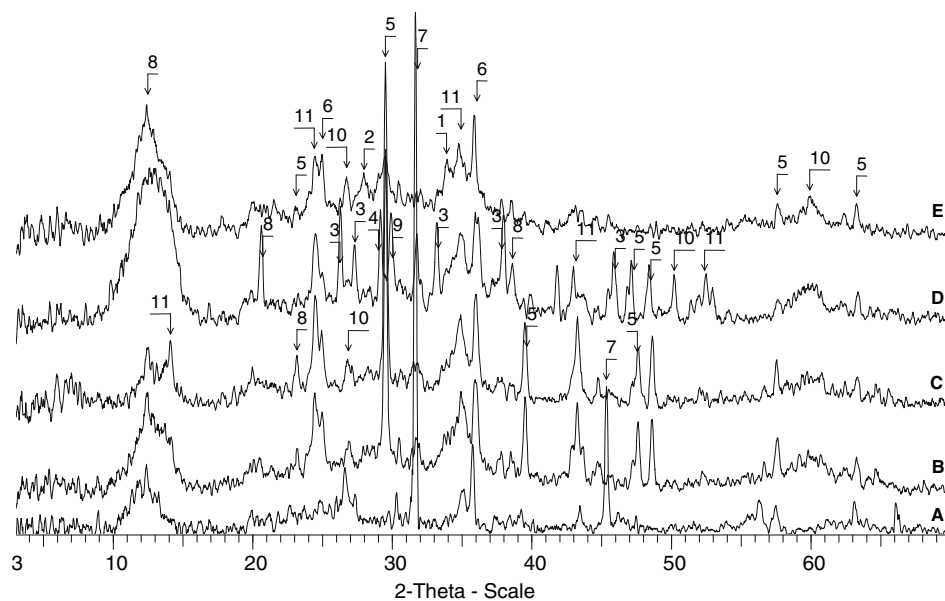
Magnesium calcite was detected in the specimens immersed in simulated acid rain and distilled water. High-magnesium calcite (CaCO₃, hexagonal-rhombohedral) is calcite with up to 23 mol% MgCO₃ in the crystal lattice. With exposure to freshwater solid particles tend merely to lose MgCO₃ and not to dissolve like aragonitic particles. Low-Mg calcite (hexagonal-rhombohedral) is calcite with less than 4 mol% MgCO₃.

Calcite, CaCO₃, is seen in the specimens immersed in seawater or subjected to weekly freeze–thaw cycles and its formation is due to the reaction of calcium oxide with atmospheric CO₂.

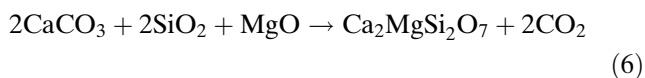
Aragonite, CaCO₃, which has the same chemistry but different crystal structure and symmetry and is less stable than calcite in most environments, is also seen in specimens immersed in seawater. Aragonite, usually converts over time to calcite and calcite pseudomorphs.

Akermanite, Ca₂MgSi₂O₇, which was seen in the outer surface of geopolymers subjected to weekly

Fig. 9 X-ray diffractograms of geopolymers tested for durability and structural integrity (A: 1N HCl solution, B: Acid rain, C: Distilled water, D: Seawater, E: Freeze–thaw cycles, 1: Akermanite, 2: Anorthite, 3: Aragonite, 4: Calcite, 5: Magnesium calcite, 6: Fayalite/Olivine, 7: Halite, 8: Kaolinite, 9: Magnetite, 10: Quartz, 11: Sodalite)



freeze–thaw cycles is a product of contact metamorphism of siliceous limestones and dolostones but can be also formed from alkalic magmas rich in calcium. In this case, it is believed that its formation is due to reaction (6), when slag particles react with sodium silicate solutions



Conclusions

This experimental study proves that geopolymers can be formed from waste materials such as low calcium ferronickel slags. The 2^3 factorial analysis shows that aging period is the factor with the most significant and positive effect on the compressive strength of the final product. All other factors, namely heating temperature and heating time as well as their interactions have either less significant or negligible effect on the final compressive strength.

Mineralogical analyses of the produced geopolymers identifies the formation of new phases, namely sodalite, maghemite, thermonatrite and trona. Sodalite is believed to be the phase that contributes most to the increased compressive strength of the final product. The formation of these phases provides useful information regarding the progress of geopolymerisation mechanisms.

The durability and structural integrity of the produced geopolymers is almost unaffected when specimens are immersed in distilled- and seawater or

subjected to freeze–thaw cycles over a period of 4 months. On the contrary, noticeable loss of strength is seen when geopolymers are immersed in 1 N HCl or simulated acid rain solutions. Mineralogical studies show the formation of phases such as halite, magnesium calcite, calcite, aragonite and akermanite on the surface of the immersed geopolymers.

A more detailed study is required in order to optimise experimental parameters and further elucidate geopolymerisation mechanisms.

Acknowledgements Assoc. Professor K. Komnitsas would like to acknowledge the financial support of the Greek Ministry of Education in the framework of PYTHAGORAS project entitled “Innovative technologies for the management of hazardous mining wastes towards prevention of groundwater contamination”, as well as LARCO S.A for providing the slag. The authors would also like to acknowledge the assistance of the laboratories of Applied Mineralogy, Rock Mechanics and Ore Processing, in various stages of this study.

References

1. European Commission – IPPC Bureau (2002) Draft reference document on best available techniques for management of tailings and waste-rock in mining activities, <http://eippcb.jrc.es/pages/Fmembers.htm>
2. Kontopoulos A, Komnitsas K, Xenidis A (1996) In: Proceedings of the IMM minerals metals and the environment II conference, Prague, September 1996, p 405
3. Davidovits J (1991) *J Ther Anal Calorim* 37:1633
4. Davidovits J (1994a) *J Mat Educ* 16:91
5. Babushkin VI, Matveyev GM, Mchedlov-Petrosyan OP (1985) *Thermodynamics of silicates*. Springer-Verlag, Berlin
6. Van Jaarsveld JGS, Van Deventer JSJ, Lukey GC (2003) *Mater Lett* 57:1272

7. Bakharev T, Sanjayan JG, Chen YB (2003) *Cement Concrete Res* 33:1607
8. Bakharev T (2005) *Cement Concrete Res* 35:658
9. Krivenko PV, Brandstetr J, Rostovskaya GS (1998) In: *Proceedings of the 6th CANMET/ACI international conference on fly ash, silica fume, slag and natural pozzolans in concrete*, Bangkok, Thailand, p 657
10. Krivenko PV, Mokhort M, Petropavlovskii O (2002) In: *Proceedings of geopolymer 2002 conference: turn potential into profit*, Melbourne, Australia
11. Palomo A, Macias A, Blanco MT, Puertas F (1992) In: *Proceedings of the 9th international congress on chemistry of cement*, New Delhi, India, p 505
12. Comrie DC, Davidovits J (1988) In: *Proceedings of the first European conference on soft mineralogy geopolymer '88*, Compiègne France (1st Edition ed.), p 125
13. Davidovits J, Comrie DC, Paterson JH, Ritcey DJ (1990) *Concr Inter* 12:30
14. Davidovits J (1994) In: *Proceedings of the first international conference on alkaline cements and concretes*, Kijev, p 131
15. Glukhovskiy VD, Rostovskaya GS, Rumyna GV (1980) In: *Proceedings of the 7th international conference on the chemistry of cement*, vol 3, Paris, France, p 164
16. Krivenko PV (2000) In: *Proceedings of the second international conference in cement and concrete in the 2000*, Istanbul, Turkey, p 553
17. Krivenko PV, Guziy SG, Titarenko TG (2005) In: *Proceedings 2nd international symposium non traditional cement and concrete*, Czech Republic
18. Van Jaarsveld JGS, Van Deventer JGJ, Lorenzen L (1997) *Miner Eng* 10:659
19. Van Jaarsveld JGS, Van Deventer JSJ, Schwartzman A (1999) *Miner Eng* 12:75
20. Xu H, Van Deventer JSJ (2000) *Int J Miner Process* 59:247
21. Davidovits J, Davidovics M (1988) *Ceram Eng Sci Proc* 9:835
22. Xu H, Van Deventer JSJ (1999) In: *Proceedings of the second international conference geopolymer '99*, France, p 43
23. Xu H, Van Deventer JSJ (2002) *Miner Eng* 15:1131
24. Phair JW, Van Deventer JSJ, Smith JD (2004) *Appl Geochem* 19:423
25. Phair JW, Van Deventer JSJ (2002) *Int J Miner Process* 66:121
26. Bakharev T (2005) *Cement Concrete Res* 35:1224
27. Fletcher RA, Mackenzie KJD, Nicholson CL, Shimada S (2005) *J Eur Ceram Soc* 25:1471
28. Weng L, Sagoe-Crentsil K, Brown T, Song S (2005) *Mat Sci Eng B Solid* 117:163
29. Van Jaarsveld JGS, Van Deventer JSJ, Lukey GC (2002) *Chem Eng J* 89:63
30. Xu H, Van Deventer JSJ, Lukey GC (2001) *Ind Eng Chem Res* 40:3749
31. Phair JW, Van Deventer JSJ (2001) *Miner Eng* 14:289
32. Lee WKW, Van Deventer JSJ (2002) *Colloid Surface A* 211:115
33. Yip CK, Lukey GC, Van Deventer JSJ (2005) *Cement Concrete Res* 35:1688
34. Cheng TW, Chiu JP (2003) *Miner Eng* 16(3):205
35. Glukhovskiy VD (1994) In: Krivenko PV (ed) *Alkaline cements and concrete*, vol 1. Vpol Stock Company, Kiev, Ukraine, p 1
36. Goretta KC, Chen N, Gutierrez-Mora F, Routbort JL, Lukey GC, Van Deventer JSJ (2004) *Wear* 256:714
37. Box GEP, Hunter WG, Hunter JS (1978) *Statistics for experimenters. An introduction to design, data analysis, and model building*. John Wiley & Sons, New York
38. Agatzini S (1981) Ph.D. Thesis, University of London
39. *Statgraphics PLUS 5 (2000) Reference Manual*. Manugistics Inc., USA
40. Zaharaki D (2004) Diploma Thesis, Department of Mineral Resources Engineering, Technical University Crete
41. Grogan KL, Gilkes RJ, Lottermoser BG (2003) *Clays Clay Minerals* 51:390
42. Madani A, Aznar A, Sanz J, Serratos JM (1990) *J Phys Chem* 94:760
43. Gadsden JA (1975) *Infrared spectra of minerals and related inorganic compounds*. Ed. Butterworths, London, UK
44. Yousuf M, Mollah A, Hess TR, Tsai Y-N, Cocke DL (1993) *Cement Concrete Res* 23:773
45. Barbosa VFF, Mackenzie KJD, Thaumaturgo C (1999) In: *Proceedings of the 2nd international conference geopolymer '99*, France, p 65
46. Socrates G (2001) *Infrared and Raman characteristic group frequencies*, 3rd edn. John Wiley & Sons Ltd., England
47. Palomo A, Blanco-Varela MT, Grazino ML, Puertas F, Vasquez T, Grutzeck MW (1999) *Cement Concrete Res* 29:997